Multifrequency Subsurface Sounding and Tomography

Konstantin P. Gaikovich
Institute for Physics of Microstructures RAS, GSP-105 Nizhniy Novgorod, Russia
Tel: +7(831)4327920, Fax: +7(831)4385553, e-mail: gai@ipm.sci-nnov.ru

ABSTRACT
A new method of the near-field electromagnetic sounding and tomography of subsurface dielectric inhomogeneities is studied. It is based on the transformation of the multifrequency inverse scattering problem to that for the complex-valued synthesized pulse. This new statement of the inverse scattering problem leads to the much better resolution of the scanning tomography based on its solution. Input data are formed by inverse Fourier transform of the scattered field spectrum measured at many frequencies in a broad frequency band at the 2D lateral scanning above the surface of an inhomogeneous medium. So, instead of the frequency dependence of data one deals with the data dependence on the pulse delay or on the corresponding effective depth of scattering. At that, obtained 2D images of such synthesized pulse are free from the noise related to the surface scattering. It makes possible to fix the region of sounded inhomogeneity much more precisely and, hence, to improve the quality of the tomography based on the solution of the inverse scattering problem in this new statement. For subsurface dielectric targets with a homogeneous internal structure, a method of their shape retrieval (computer holography) is demonstrated.

Keywords: tomography, electromagnetic sounding, inverse scattering problem.

1. INTRODUCTION

The proposed method overcomes existing problems of the near-field scanning tomography [1] using the possibility to transform the multifrequency inverse scattering problem to that in the time domain. To obtain tomograms, 2D measurements along the interface of the sounded region should be carried out while depending on a third parameter that determines the depth sensitivity (such as signal frequency, probe altitude or its size). The statement of 3D inverse scattering problems is typically based on the solution of 3D integral equations of the 1st kind. It leads to limitations of the grid size used at calculations and, hence, to the limitation of the achievable resolution. Another limitation is related to the Rayleigh resolution limit. These limitations could be overcome on the basis of the near-field approach developed in [1]. In this paper, it was proposed to reduce 3D inverse problems for near-field measurements to the solution of one-dimensional integral equations by the 2D inverse Fourier transform over transversal co-ordinates.

This approach has been developed further in the solution of the near-field inverse scattering problem for the scanning tomography of inhomogeneities in arbitrary multilayer media using the proposed method of data acquisition [2]: it involves in an analysis 2D lateral distribution of the scattered field measured by the scanning at the unchanging source-receiver relative position. Necessary Green functions have been obtained using the plane wave decomposition of fields and, to retrieve 3D complex-valued permittivity distributions from the solution of Fredholm integral equations of the 1st kind, algorithms based on the generalized discrepancy principle in the complex Hilbert space W_2^1 have been worked out. This theory has been applied by us to develop the multifrequency microwave tomography of subsurface dielectric inhomogeneities [3], however, the scattering by surface inhomogeneities leads to so high noise level that it is difficult to discern the contribution of subsurface targets in the signal. Finally, to overcome this difficulty, the new approach based on the transformation of the multifrequency inverse scattering problem to that for a synthesized pulse has been proposed and applied in [4], and this approach is studied here in the numerical simulation. Also, simulation results for targets with a homogeneous internal structure are used to retrieve their shape, *i.e.*, to demonstrate the feasibility of the near-field computer holography.

2. THEORY

Following [1-4], let us consider a scattering region with the complex permittivity $\varepsilon(\mathbf{r}) = \varepsilon_0 + \varepsilon_1(\mathbf{r})$ that is embedded in a half-space $z \le 0$ with $\varepsilon = \varepsilon_0$. The total field at the frequency ω is a sum of probing and scattered field components $\mathbf{E}(x, y, \omega) = \mathbf{E}_0(x, y, \omega) + \mathbf{E}_1(x, y, \omega)$. For the scheme of measurements with the fixed source-receiver vector $\boldsymbol{\delta}\mathbf{r}$, when the structure of the probing field is invariable relative to the receiver position, it is possible to express the *k*-space spectrum (2D inverse Fourier transform over *x* and *y*) of the scattered field in frameworks of the Born approximation [2]:

$$E_{1i}(\omega,k_x,k_y,z,\boldsymbol{\delta}\mathbf{r}) = -4\pi^3 i\omega \int_{z'} \varepsilon_1(k_x,k_y,z')[\int_{-\infty}^{\infty}\int_{-\infty}^{\infty} \mathrm{e}^{-i\kappa_x\delta x - i\kappa_y\delta y}$$
$$\times \int_{z''} [j_i(\omega,\kappa_x,\kappa_y,z''-z-\delta z) G_{ij}^{12}(\omega,\kappa_x,\kappa_y,z'',z')] G_{ji}^{21}(\omega,\kappa_x+k_x,\kappa_y+k_y,z',z) d\kappa_x d\kappa_y dz'' dz', \quad (1)$$

$$G_{ji}^{12}(k_x,k_y,z'',z') = -\frac{1}{2\pi\omega}\frac{k_0^2}{k_\perp}\exp i\left\{-\sqrt{k_1^2-k_\perp^2}\,z'' + \sqrt{k_2^2-k_\perp^2}\,(z'-d) - \sqrt{k_2^2-k_\perp^2}\,d\right\}$$
$$\times[\frac{1}{k_1 k_2} T_{12}^{\parallel} \begin{Vmatrix} \frac{k_x^2 k_{z2}}{k_\perp} & \frac{k_x k_y k_{z2}}{k_\perp} & -k_x k_\perp \\ \frac{k_x k_y k_{z2}}{k_\perp} & \frac{k_y^2 k_{z2}}{k_\perp} & -k_y k_\perp \\ -\frac{k_x k_\perp k_{z2}}{k_{z1}} & -\frac{k_x k_\perp k_{z2}}{k_{z1}} & \frac{k_\perp^3}{k_{z1}} \end{Vmatrix} + \frac{1}{k_{z1}k_\perp} T_{12}^{\perp} \begin{Vmatrix} k_y^2 & -k_x k_y & 0 \\ -k_x k_y & k_x^2 & 0 \\ 0 & 0 & 0 \end{Vmatrix}],$$

$$G_{ji}^{21}(k_x,k_y,z',z) = -\frac{1}{2\pi\omega}\frac{k_0^2}{k_\perp}\exp i\left\{-\sqrt{k_1^2-k_\perp^2}\,z + \sqrt{k_2^2-k_\perp^2}\,(z'-d) - \sqrt{k_2^2-k_\perp^2}\,d\right\}$$
$$\times[\frac{1}{k_1 k_2} T_{21}^{\parallel} \begin{Vmatrix} \frac{k_x^2 k_{z1}}{k_\perp} & \frac{k_x k_y k_{z1}}{k_\perp} & k_x k_\perp \\ \frac{k_x k_y k_{z1}}{k_\perp} & \frac{k_y^2 k_{z1}}{k_\perp} & k_y k_\perp \\ \frac{k_x k_\perp k_{z1}}{k_{z2}} & \frac{k_y k_\perp k_{z1}}{k_{z2}} & \frac{k_\perp^3}{k_{z2}} \end{Vmatrix} + \frac{1}{k_{z2}k_\perp} T_{21}^{\perp} \begin{Vmatrix} k_y^2 & -k_x k_y & 0 \\ -k_x k_y & k_x^2 & 0 \\ 0 & 0 & 0 \end{Vmatrix}].$$

where $k_0 = \omega/c$, $k_\perp^2 = k_x^2 + k_y^2$, G_{ji}^{lk} are *k*-space components of Green tensors; j_i is the *k*-space source current distribution (for brevity we use same notations for *k*-space representations). Variations of complex amplitudes of the received signal *s* are expressed by the convolution of the instrument function **F** of the receiver and the scattered field $\mathbf{E_1}$:

$$s(\mathbf{r}_r) = \int \mathbf{E}_1(\mathbf{r}')\mathbf{F}(x_r - x', y_r - y', z_r, z')dx'dy'dz' \quad (2)$$

where $\mathbf{r}_r$ is the vector determining the receiver position. From (1) and (2), the transversal spectrum of measured signal variations is obtained as:

$$s(k_x,k_y,\omega) = \int_{z'} \varepsilon_1(k_x,k_y,z')K(k_x,k_y,z',\omega)dz' \quad (3)$$

This equation has been used in our algorithm of the microwave subsurface tomography [3]; but it was difficult to recognize sounded subsurface objects on the measured image of $s(x,y,\omega)$ against the noise produced by the surface scattering. However, we have found [4] that it is possible to obtain much better images of subsurface targets, using the transformation of multifrequency data to synthesized pulse. It suggests that we make similar transformations in Equation (3) [4]:

$$s(k_x,k_y,t) = \int_0^\infty s(k_x,k_y,\omega)\exp(i\omega t)d\omega \quad (4)$$

that can be represented in dependence on the effective depth parameter z_s according $s(k_x,k_y,z_s) = s(k_x,k_y,t = z_s \operatorname{Re}\sqrt{\varepsilon_0}/c)$ that leads to the new equation that relates the complex permittivity spectrum to the complex-valued synthesized pulse of the signal lateral spectrum:

$$s(k_x,k_y,z_s) = \int_{z'} \varepsilon_1(k_x,k_y,z')K(k_x,k_y,z',z_s)dz' \quad (5)$$

$$K(k_x,k_y,z',z_s) = K(k_x,k_y,z',t = z_s \operatorname{Re}\sqrt{\varepsilon_0}/c),\ K(k_x,k_y,z',t) = \int_0^\infty K(k_x,k_y,z',\omega)\exp(i\omega t)d\omega$$

The depth dependence of $K(k_x,k_y,z',z_s)$ in Equation (5) has maxima at depths z' that are placed deeper with the increase of $|z_s|$ – unlike the kernel of (3) that has maxima near the surface. It can explain the observed depth selectivity and resolution of such pseudopulse images as well as the absence of noise related to the surface

scattering. Also, as it is well-known [5] that kernels with maxima, such as in Equation (5), provide better solution results in comparison with the exponential kernel of the initial Equation (3).

To solve the Fredholm integral equation, the algorithm based on the generalized discrepancy principle in the complex Hilbert space W_2^1 [2] has been applied here to retrieve tomography images of subsurface inhomogeneities with the complex-valued distribution of permittivity. From the solution of (5), the desired 3D structure of permittivity (tomogram) is obtained by the 2D inverse Fourier transform:

$$\varepsilon_1(x,y,z) = \iint \varepsilon_1(\kappa_x,\kappa_y,z)\exp(i\kappa_x x + i\kappa_y y)d\kappa_x d\kappa_y \tag{6}$$

In practice, subsurface targets mostly have a homogeneous internal structure. When it is known *a priori* that the permittivity of a target $\varepsilon_1^0 = const$, the tomography problem can be reduced to the problem of the target shape retrieval, *i.e.* to the problem of the computer holography. For that, the k-space permittivity spectrum can be written as a Fourier transform with finite limits [4]:

$$\varepsilon_1(k_x,k_y,z) = \frac{1}{4\pi^2}\int_{y_1}^{y_2}\int_{x_1(y)}^{x_2(y)} \varepsilon_1^0 e^{-ik_x x - i\kappa_y y}dxdy = \frac{\varepsilon_1^0}{4\pi^2}\int_{y_1}^{y_2}\exp(-i\kappa_y y)\frac{1}{ik_x}(e^{-ik_x x_1(y)} - e^{-ik_x x_2(y)})dy. \tag{7}$$

Then, making the inverse Fourier transform of (9) over k_y, obtain the complex-value transcendent equation:

$$\varepsilon_1(k_x,y',z) = \int_{-\infty}^{\infty}\varepsilon_1(k_x,k_y,z)\exp(ik_y y')dk_y = \frac{\varepsilon_1^0}{2\pi ik_x}(e^{-ik_x x_1(y',z)} - e^{-ik_x x_2(y',z)}) \tag{8}$$

that is equivalent to the system of two real equations. The desired shape of the target expressed by two functions $x_1(y,z)$, $x_2(y,z)$ is obtained from this equation, using the solution $\varepsilon_1(k_x,k_y,z)$ of Equation (5). It should be mentioned that this equation is overdetermined: it can be solved at each value of k_x.

3. NUMERICAL SIMULATION

To simulate the proposed tomography quite generally, all spatial sizes is given further in units of the lower wavelength λ_{min} in analysis. At that, the case, considered in [4], is reproduced at $\lambda_{min} = 4$ cm. Multifrequency measurements of signal complex amplitudes are simulated in the wavelength band 1-4 (in our relative wavelengths units). It is assumed that they are obtained by 2D lateral scanning in the rectangle *x*-*y* area with sizes 7.5×5 above targets buried in a media with $\varepsilon_0 = 4 + i$. The considered source-receiver system includes two identical transmitting and receiving antennas placed in *y*-direction with sizes 0.75×1. They were scanning together the fixed distance between their centers $\Delta y = 1.8$. In Fig. 1 kernels of Equations (3) and (5) are shown for a pair of components of their lateral spectra.

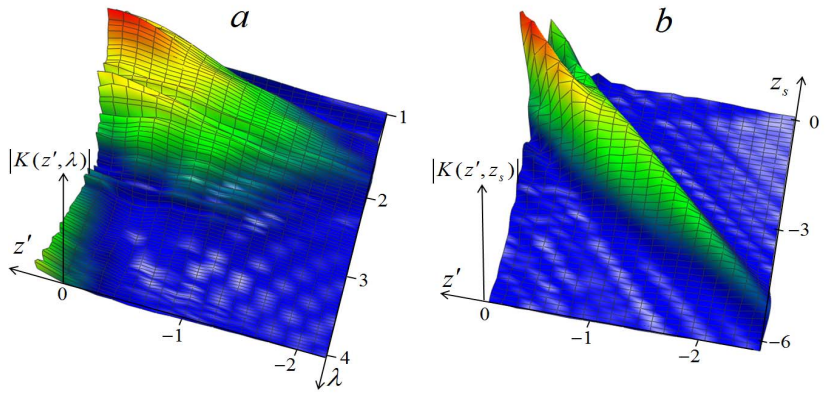

Figure 1: (a) spectral component of the kernel of equation (3); (b) corresponding kernel of (5).

It is easily seen that the near-surface contribution of the kernel (3) in the signal is dominated at each separate frequency (that makes it difficult to discern the field scattered by deep targets from the noise introduced by surface inhomogeneities – as it has been demonstrated in measurements [4]), whereas the kernel of (5) for the synthesized pulse have maxima at various depths throughout the interval of sounding.

In the simulation of tomography, signal complex amplitudes at 81 wavelengths in the region of 1-5 with the random gauss-distributed noise at *rms* 5% have been used in the analysis. They have been calculated for the system of two identical transmitting and receiving antennas (with sizes 1×0.75 at the fixed distance between their centers of 1.8 and a homogeneous distribution of the current $\mathbf{j} = j_y\mathbf{y}$) placed in the *y* direction and scanning together in the rectangle *x*-*y* area with sizes 7.5×5 above buried targets. In Fig. 2a,b, tomography results for the

real part of the sample permittivity are shown for a parallelepiped sample $\varepsilon_1^0(\mathbf{r}) = 3 + i$ with sizes $1 \times 0.75 \times 0.5$ buried at depth $z = -1$ (similar to that, studied in [4]). Corresponding holography images obtained by the retrieved *k*-space permittivity $\varepsilon_1(k_x, k_y, z)$ from the solution of (8) are presented in Fig. 2c,d.

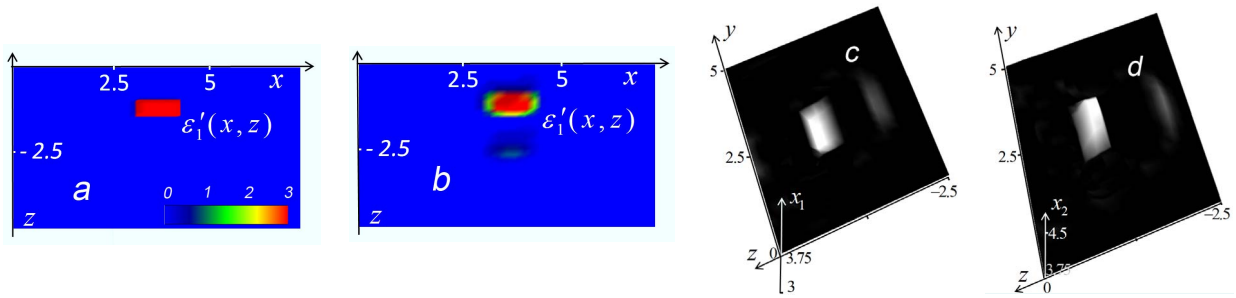

Figure 2. Results of subsurface tomography: (a) Simulated target (real part) in vertical section at y = 2.5; (b) Result of tomography; (c,d) Holography images of the target shape obtained as functions $x_1(y,z)$, $x_2(y,z)$.

Results for the imaginary part of permittivity are similar. One can in Fig. 2 that results of tomography and holography simulation are in a good correspondence with parameters of simulated target. Of course, like in every ill-posed problem [5], the solution should be based on the especial numerical modelling in each case; moreover, it should be based on the experimental study of similar cases because it is uneasy to estimate errors related to Born approximation theoretically, as well the accuracy of possible corrections to this approximation, proposed in [2] and applied in the solution of the considered tomography problem in [4]. Taking into account these theoretical and experimental difficulties, results demonstrate rather the achievable quality of the proposed methods of near-field tomography and holography in their further development.

4. CONCLUSIONS

Obtained results validate the experimental study [4] of this tomography method that can be applied in various applications of electromagnetic or acoustic physical diagnostics, including biomedical diagnostics of tumors, defectoscopy, civil engineering, anti-personnel mine detection, and underground remote sensing.

ACKNOWLEDGEMENTS

This work was supported by Russian Foundation for Basic Research (grant *No*. 12-02-90028_Bel) and by the Program of Physical Sciences Department of the Russian Academy of Sciences.

REFERENCES

[1] Gaikovich K.P.: Subsurface near-field scanning tomography, *Physical Review Letters*, **98**, 183902, 2007.
[2] Gaikovich K.P., Gaikovich P.K.: Inverse problem of near-field scattering in multilayer media. *Inverse Problems*, **26**, no.12, 125013, 2010.
[3] Gaikovich K.P., Gaikovich P.K., Maksimovitch Ye.S., Badeev V.A.: Multifrequency microwave tomography of absorbing inhomogeneities, in *Proc. 5th International Conference "Ultrawideband and Ultrashort Impulse Signals"*, Sevastopol, Ukraine, Sept. 6-10, 2010, p. 156.
[4] Gaikovich K.P., Gaikovich P.K., Maksimovitch Ye.S., Badeev V.A.: Pseudopulse near-field subsurface tomography, *Physical Review Letters*, **108**, 163902, 2012.
[5] Gaikovich K.P. *Inverse Problems in Physical Diagnostics*. New York: Nova Science Publishers Inc., 2004.